Fish and Shellfish Immunology 170 (2026) 111119

Contents lists available at ScienceDirect

Fish and Shellfish Immunology

journal homepage: www.elsevier.com/locate/fsi

Full length article

Combined effects of temperature and metals on immunity of juveniles of European oyster *Ostrea edulis*

Halina Falfushynska [a], Dominique Noetzel [b,c], Bernd Sures [d,e], Milen Nachev [d], Bernadette Pogoda [c], Bérenger Colsoul [f], Inna M. Sokolova [b,g,*]

[a] Anhalt University of Applied Sciences, Köthen, Germany
[b] Department of Marine Biology, Institute for Biological Sciences, University of Rostock, Rostock, Germany
[c] Department of Shelf Seas Systems Ecology, Alfred-Wegener-Institute Helmholtz Center for Polar and Marine Research, Bremerhaven, Germany
[d] Aquatic Ecology and Centre of Water and Environmental Research (ZWU), University of Duisburg-Essen, Essen, Germany
[e] Research Center One Health Ruhr, University Alliance Ruhr, Faculty of Biology, University of Duisburg-Essen, Essen, Germany
[f] Thünen Institute of Fisheries Ecology, Bremerhaven, Germany
[g] Department of Maritime Systems, Interdisciplinary Faculty, University of Rostock, Rostock, Germany

A B S T R A C T

The European flat oyster (*Ostrea edulis*) is a foundational ecosystem engineer that has suffered widespread population declines due to overfishing, habitat degradation, and disease. Effective restoration requires understanding how environmental stressors impact juvenile oysters, a critical life stage for survival and recruitment. While trace metals such as zinc (Zn) and copper (Cu) are essential micronutrients, elevated concentrations can disrupt cellular physiology and immune function, particularly under temperature fluctuations associated with climate change. In this study, we investigated the combined effects of dissolved Zn (100 and 1000 μg L^{-1}) and Cu (10 and 100 μg L^{-1}) at three temperatures (5 °C, 15 °C, 22 °C) on immune defenses in juvenile *O. edulis*. Baseline tissue concentrations in controls were 73.0 ± 9.5 μg g^{-1} Cu and 1240.5 ± 113.7 μg g^{-1} Zn and were unaffected by temperature. Low metal exposures did not alter tissue concentrations, whereas high exposures induced temperature-dependent accumulation, peaking at 22 °C (CuH: 381.9 ± 78.6 μg g^{-1}; ZnH: 4573.6 ± 603.8 μg g^{-1}). Temperature strongly modulated cellular immunity: hemocyte abundance was highest at 15 °C, phagocytosis and acid phosphatase activity increased at 22 °C, while lipid peroxidation levels were elevated at 5 °C and 22 °C, indicating stress-induced responses at thermal extremes. Zn stimulated acid phosphatase but suppressed phenoloxidase activity, whereas Cu increased hemocyte mortality and modestly stimulated phenoloxidase. Lysozyme activity was elevated at cold exposure (5 °C), suggesting enhanced antibacterial defenses. Multivariate PLS-DA analyses revealed clearer separation of immune profiles by temperature than by metal exposure. These results demonstrate that temperature is the dominant factor shaping immune competence in juvenile *O. edulis*, while metal contamination at environmentally realistic levels exerts only minor effects, with implications for restoration and management under climate change.

1. Introduction

Marine bivalves, including the European flat oyster (*Ostrea edulis*), function as essential ecosystem engineers, contributing significantly to habitat formation, water quality regulation, and biogeochemical cycling [1,2]. Through their filter-feeding activity, they play a key role in trophic webs by controlling phytoplankton abundance, while their physical structures enhance biodiversity by providing habitat and substrate stabilization. Oyster reefs also improve coastal resilience by reducing shoreline erosion and mitigating the effects of extreme weather events [3]. Moreover, *O. edulis* and other bivalves are important aquaculture species, supporting the blue economy and contributing to food security [4–6].

Pathogens and parasites represent major sources of mortality in both wild and aquacultured populations of marine bivalves [7]. As filter feeders with long lifespans, bivalves are continuously exposed to diverse microorganisms in seawater and sediments [8]. Their defense relies on an innate immune system, which depends critically on hemocytes, the circulating blood cells that form the main cellular component of the hemolymph [9]. Hemocytes orchestrate innate immune defenses and support key physiological processes, including nutrient transport, wound healing, detoxification, and shell mineralization [10–12]. They mediate core effector functions such as phagocytosis, encapsulation, and the production of cytotoxic molecules and signaling factors, so that their composition and functional status closely reflect the animal's overall physiological and immunological condition [9–11]. The ecological and economic roles of bivalves are increasingly threatened by environmental stressors, including metal pollution and warming, which can

* Corresponding author. Department of Marine Biology, Institute for Biological Sciences, University of Rostock, Rostock, Germany.
E-mail address: inna.sokolova@uni-rostock.de (I.M. Sokolova).

https://doi.org/10.1016/j.fsi.2026.111119
Received 18 September 2025; Received in revised form 30 December 2025; Accepted 8 January 2026
Available online 9 January 2026

compromise hemocyte function and weaken immune defenses. Outbreaks of infectious diseases are expected to become more frequent under global climate change, driven by increased pathogen spread and proliferation, as well as suppression of bivalve immune function by prolonged or extreme heat exposure [13–15]. In addition, urbanization and pollution may further exacerbate disease risks by enhancing pathogen exposure and weakening immune defenses [7,16].

Immune function in bivalves is highly sensitive to environmental stressors including temperature and pollution [17–19]. Mild warming within species-specific optimal ranges can enhance immune responses, whereas temperature extremes or prolonged suboptimal exposure suppress immunity and increase pathogen vulnerability [13,16,20,21]. Immune parameters are among the earliest and most sensitive indicators of metal pollution [22–24], and hemocytes are particularly sensitive to metals and temperature stress [10,25–28]. In adults, exposure to metals such as Cd and Cu, or metal-containing nanoparticles, induces oxidative stress, disrupts immune gene expression, impairs hemocyte functions including phagocytosis, and can trigger apoptosis [22,29–33]. Metals may also enrich microbial communities with antibiotic resistance genes, further increasing disease susceptibility [34]. Moreover, elevated temperatures can alter the toxicokinetics of contaminants, often enhancing metal uptake while exerting less influence on elimination processes [35–37]. This imbalance may lead to increased internal metal burdens, inducing oxidative stress and impairing immune competence. However, little is known about the combined effects of metals and temperature on juvenile oyster immunity. Understanding these interactions is critical for optimizing hatchery conditions, guiding restoration strategies, and improving resilience assessments in a changing climate [38–40].

The European flat oyster *O. edulis* once thrived across European seas but has suffered dramatic population declines due to overfishing, disease, invasive species, and pollution [40–43]. Restoration initiatives, such as the RESTORE and DAM CREATE projects, seek to reestablish this ecologically vital species in the North Sea [44–46] and highlight the importance of understanding how environmental stressors affect the performance and health of juvenile oysters commonly used in restoration efforts. While bivalve larvae have shown high sensitivity to temperature and metal pollution, with both warming and metal contamination implicated in hatchery failures [38,39,47], adult oysters exhibit greater tolerance [48–50]. However, little is known about the sensitivity of *O. edulis* juveniles to trace metals, particularly under varying temperatures. This developmental stage is critical for maturation and growth, and exposure of juveniles to the combined temperature and pollution stress might affect their fitness and performance as adults [51–53]. Given the increasing prevalence of multi-stressor environments, assessing the interactive effects of temperature and metal exposure on *O. edulis* juveniles is essential for informing conservation strategies and ensuring the long-term success of restoration efforts [54].

This study aimed to investigate the combined effects of dissolved trace metals (zinc, Zn, and copper, Cu) and temperature (5 °C, 15 °C, and 22 °C) on the immune defense of juvenile *O. edulis*. Both Zn and Cu are essential metals acting as cofactors of multiple enzymes and transcription factors, but they are toxic when present in excess due to the induction of oxidative stress, metabolic dysregulation and cell death [55–57]. Furthermore, while dissolved Cu and Zn exhibit toxic effects on pathogens [58,59], their bactericidal properties may be outweighed by their detrimental impact on hemocyte survival and function, ultimately leading to a net immunosuppressive effect [22,24,32,58]. Here, we hypothesized that environmentally realistic levels of Zn and Cu contamination would induce oxidative damage, as well as negatively impact hemocyte viability, function, and the activity of immune-related enzymes in *O. edulis* juveniles. Additionally, we hypothesized that temperatures exceeding the typical environmental range (22 °C) would exacerbate metal immunotoxicity. To test these hypotheses, we exposed juvenile *O. edulis* to different concentrations of Zn and Cu for three weeks and evaluated immune responses encompassing both cellular and humoral components.

2. Materials and methods

Oyster maintenance and experimental exposures. European flat oysters (*O. edulis*) originated from the Seasalter (Walney) Ltd. oyster hatchery (54°3′0.16″ N, 3°11′10.57″ W) in Morecambe Bay (Irish Sea), north-west England. All 800 juvenile oysters used in this study came from a single hatchery batch and were of similar size and age. Prior to transport to the University of Rostock, the oysters were maintained in commercial oyster baskets (SEAPA, Australia) within a 4500 L tank connected to a flow-through system at the Helgoland Oyster Hatchery (54°10′39.68″ N, 7°53′30.45″ E), operated by the Alfred-Wegener-Institute (AWI). The juvenile status of the oysters was confirmed based on both the immature gonadal condition observed upon dissection and their morphometric characteristics. A random subset of 30 oysters had a mean length of 24.3 ± 3.1 mm (ventral–dorsal distance), a height of 28.7 ± 3.2 mm (umbo to distal shell margin), a width of 8.4 ± 1.2 mm, and a total wet mass (including shell) of 3.0 ± 0.8 g. In April and June, two batches of 400 juvenile oysters were transported from the AWI to the University of Rostock, wrapped in moistened fabric with cooling packs placed above and below within a 20 L insulating box (Thermo Future Box®, Germany). No mortality occurred during the one-day transport. The oysters retained their juvenile status throughout the experiment, as confirmed by dissection at its conclusion.

Oysters were allocated to three circular tanks, each containing approximately 50 L of artificial seawater (salinity: 32 ± 1). Artificial seawater was prepared by mixing deionized water from an ion exchanger (Orben Ministil P 102, Germany) with a conductivity of ~1.7 μS cm^{-1} and sea salt (Pro Reef Sea Salt, Tropic Marin, Germany). Oysters were maintained at temperatures ranging from 10 °C to 13 °C, reflecting Helgoland temperature conditions in April and June, respectively. Water was filtered during the day using an external filter (EHEIM Experience 150, Germany). Oysters were fed daily in the evening with 300 μL g^{-1} wet weight of Shellfish Diet 1800® (Reed Mariculture, USA), an instant microalgae mixture comprising *Isochrysis* sp., *Pavlova* sp., *Tetraselmis* sp., *Thalassiosira weissflogii*, and *Thalassiosira pseudonana*. During nighttime, filters were deactivated to minimize microalgae removal, while water circulation was maintained using water pumps (Eheim compactOn 1002). The timeline of acclimation, warming/cooling, and experimental exposures to different temperature and metal regimes is shown in Fig. 1.

Following a two-week acclimation period in artificial seawater, 120 oysters per temperature condition were distributed among five 5 L polypropylene (PP) buckets, each containing 3 L of artificial seawater (salinity: 32 ± 1) and aerated with air pumps (Eheim Air 200, Germany). Temperature was adjusted within one week to target values of 5 °C, 15 °C, and 22 °C, based on the seasonal mean water temperatures recorded at the pilot oyster restoration site at Borkum Reef Ground between September 2017 and September 2018. The mean spring temperature was 5.7 °C, summer temperature reached 14.9 °C, autumn temperature was 16.8 °C, and winter temperature averaged 6.7 °C [54]. Two lower temperature treatments (5 °C and 15 °C) were selected to represent the mean temperatures of spring and summer, respectively, while the elevated temperature (22 °C) was chosen to simulate an extreme warming scenario. A water-cooled chest (Haake A 25B, Thermo Scientific) was used for the 5 °C treatment, a cold storage unit (Viessmann TE 1500/2250/100) for the 15 °C treatment, and a water bath (Haake A10, Thermo Scientific) for the 22 °C treatment. Oysters remained at the respective temperature for one additional week to ensure acclimation.

Following acclimation, oysters were distributed evenly (8 oysters per bucket) across 15 randomly placed buckets, each containing 2 L of artificial seawater. Zinc chloride ($ZnCl_2$) was added at nominal concentrations of 100 μg L^{-1} (ZnL treatment) and 1000 μg L^{-1} (ZnH treatment) to five buckets each, while five buckets served as untreated controls. Copper exposure experiments followed the same procedure, with nominal concentrations of 10 μg L^{-1} (CuL treatment) and 100 μg L^{-1} (CuH treatment). Water changes and metal re-spiking were

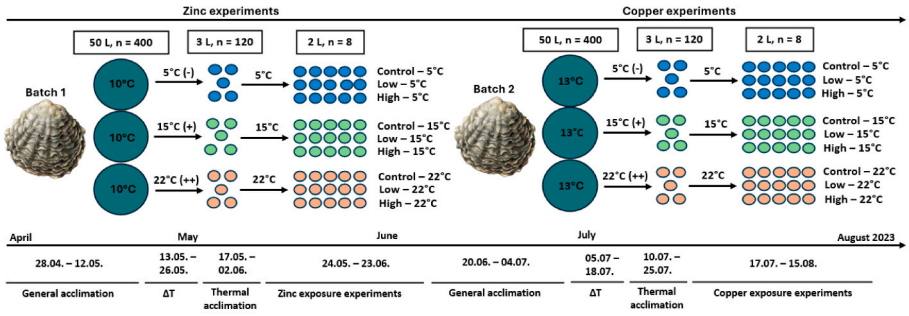

Fig. 1. Schematic of the experimental design and timeline.
n – housing density. Control – exposure without added metals; Low – exposure to low metal concentrations (nominally 100 μg L^{-1} Zn or 10 μg L^{-1} Cu); High – exposure to high metal concentrations (nominally 1000 μg L^{-1} Zn or 100 μg L^{-1} Cu).

performed every 48 h. Oysters were fed daily with 300 μL g^{-1} wet weight of Shellfish Diet 1800®. Temperature was monitored daily (Ebro TFX 410-1 Pt1000, Germany), while salinity and oxygen saturation were measured bi-daily using a multimeter (Hach HQ 40d, Germany) (Table 1). Each exposure experiment lasted three weeks per temperature and metal treatment. At the end of the three-week exposure period, hemolymph was collected for the assessment of the immune parameters, and whole-body tissues were sampled and shock-frozen for metal analysis.

Water sampling. Water samples (50 mL) were collected during every second water change from each experimental treatment, alternating between periods immediately before and after water changes to capture temporal variations in metal concentrations. Prior to sampling, thorough mixing was conducted to ensure homogeneity. For metal analysis, water samples were taken from one randomly selected replicate bucket (out of five) per experimental exposure condition, collected in 50 mL conical tubes, and immediately frozen at −20 °C. Before metal analysis, the samples were thawed, filtered through 45 μm filters, and acidified with metal-grade HNO_3 (1 % final concentration).

Metal analyses. For the Cu and Zn analysis, the water and oyster whole-body samples were prepared and processed as described in Janardhanan et al. [60]. Briefly, oyster whole soft body was digested in 4 mL 65 % nitric acid (HNO_3, subboiled) using a Mars 6 microwave digestion system (CEM Corporation, Kamp-Lintfort, Germany). The tissue dry mass used for metal analysis (mean ± SEM) was 56.2 ± 2.9 mg in the Zn exposure experiments (N = 72) and 46.3 ± 3.2 mg in the Cu exposure experiments (N = 72). Subsequently, all samples were diluted 1:10 with an internal standard solution (1 % HNO_3 containing scandium as the internal standard) and analyzed using a quadrupole inductively coupled plasma mass spectrometer (ICP-MS, PerkinElmer NexION 2000, PerkinElmer Corporation, Waltham, USA) operating in standard mode at 1500 W plasma power, 16 L/min plasma gas flow, and 1.02 L/min nebulizer gas flow. Concentrations of metals in the water and oyster tissue were calculated in μg/L and μg/g, respectively, based on the slopes of regression lines obtained from instrument calibration (for further details, see Ref. [60]).

The accuracy analytical procedure was controlled using the standard reference material 1566b-Oyster Tissue (National Institute of Standards and Technology, NIST), whereas the obtained recovery rates were in the range ±20 %. Due to technical challenges and mass interferences during Cu quantification in the seawater matrix resulting in discrepancies between the ^{63}Cu and ^{65}Cu isotopic signals, Cu concentrations in the water could not be reliably reported. This problem, however, did not affect Cu measurements in oyster tissues. Zinc concentrations were reliably quantified in both the seawater and tissue matrices.

Hemolymph collection. Hemolymph was aseptically collected from the adductor muscle of oysters using a sterile syringe with a 23-gauge needle and immediately mixed with hemocyte extraction buffer (pH 7.3) at a 2:1 (vol:vol) ratio. The buffer consisted of 20 mM HEPES, 436 mM NaCl, 53 mM $MgSO_4$, 10 mM $CaCl_2$, and 10 mM KCl. A small aliquot of each sample was visually inspected under a microscope to determine hemocyte concentration and assess sample quality. The hemolymph appeared clear and showed no signs of contamination or coagulation. Each biological replicate consisted of hemolymph pooled from three oysters. Hemocytes were isolated by centrifuging the hemolymph at 600×*g* for 10 min, followed by resuspension of the resulting pellet in 0.2 mL of artificial seawater. The hemocyte concentration in the hemolymph was quantified using a BrightLine hemocytometer (Fisher Scientific GmbH, Schwerte, Germany). Cell viability was assessed using the Trypan Blue exclusion method, where non-viable cells were identified by blue staining. Mortality was calculated as the proportion of stained (dead) hemocytes relative to the total hemocyte count. Due to the sample loss, hemocyte mortality data are not available for the Zn exposure experiment.

Assessment of the immune parameters. Phagocytic activity was determined as described elsewhere [24,61]. Hemocytes (mean ± SEM: 0.316 ± 0.013 × 10^6 cells per sample; N = 108) were incubated with zymosan particles at 18 °C for 30 min, followed by washing and extraction of Neutral Red dye from engulfed particles using 1 % acetic acid in 50 % ethanol for 5 min. The phagocytic index was established as the number of ingested zymosan particles per cell based on the absorbance of Neutral Red at 550 nm.

Oxidative stress was assessed by quantifying thiobarbituric acid reactive substances (TBARS) in hemocyte suspensions at 532 nm [62]. TBARS levels serve as a proxy for lipid peroxidation (LPO) resulting from the oxidation of polyunsaturated fatty acids and reflecting the balance between production and antioxidant-mediated detoxification of reactive oxygen species (ROS) in hemocytes [63]. The LPO levels were calculated using a molar extinction coefficient of 1.56 × 10^5 M^{-1} cm^{-1} and expressed as μmol·10^6 $cells^{-1}$.

To evaluate reactive nitrogen species, the concentrations of nitric oxide (NO) metabolites (nitrite and nitrate) were determined spectrophotometrically at 540 nm using the Griess reaction [64]. Vanadium (III) chloride served as the reducing agent, and a sodium nitrite standard

Table 1
Temperature, salinity and oxygen saturation of the artificial seawater during the trace metal experiments (mean ± SD).
Temperatures were measured daily, salinity and oxygen saturation every second day before the water change.

Metal	Temperature [°C]	Salinity	Oxygen [% air]
Zinc	5.3 ± 0.5	31.4 ± 0.3	91.7 ± 4.1
	14.8 ± 0.4	32.5 ± 0.4	97.9 ± 2.6
	22.1 ± 0.3	32.9 ± 0.3	98.5 ± 3.3
Copper	5.0 ± 0.7	32.1 ± 0.5	97.5 ± 3.4
	15.0 ± 0.2	32.4 ± 0.3	100.2 ± 3.1
	21.9 ± 0.3	33.0 ± 0.6	101.2 ± 2.3

curve was used for quantification. The NO levels were reported in μmol·10^6 $cells^{-1}$.

Lysosomal function was evaluated via acid phosphatase (AP) activity following the protocol outlined by Walter and Schütt [65]. The assay was conducted in 50 mM Na-citrate buffer (pH 4.8) containing 5.5 mM p-nitrophenyl phosphate at 18 °C. The hydrolysis reaction's product was measured at 405 nm, with enzyme activity expressed as μmol·min^{-1}·10^6 $cells^{-1}$, applying a molar extinction coefficient of 18.5 × 10^3 M^{-1} cm^{-1} for p-nitrophenol.

Phenoloxidase-like (PhO) activity was determined in hemolymph plasma by monitoring o-quinone formation at 420 nm using p-phenylenediamine as a substrate at a final concentration of 50 mM [66]. The reaction was analyzed using a molar extinction coefficient of 43,160 M^{-1} cm^{-1} and expressed as nmol o-quinones produced·min^{-1}·ml.

The enzymatic activity of lysozyme (LYZ) in hemolymph plasma was determined using a turbidimetric assay based on the lysis of *Micrococcus lysodeikticus* cell suspension [67]. The decrease in absorbance at 450 nm was measured spectrophotometrically over time. The assay was conducted in a phosphate buffer (pH 6.24) at 25 °C, with enzyme activity calculated based on the rate of absorbance reduction. One unit of lysozyme activity was defined as the amount of enzyme causing a decrease in absorbance of 0.001 per minute under the specified conditions.

Statistical analysis. The data were tested for normal distribution using the Shapiro–Wilk test and for homogeneity of variances using Levene's test, with Bonferroni corrections. For data that met the assumptions of parametric analysis, a two-way analysis of variance (ANOVA) was conducted, followed by Tukey's Honest Significant Difference (HSD) post-hoc test. Temperature (three levels) and metal exposure (three levels) were treated as fixed factors. Analyses were performed separately for the Zn and Cu exposure experiments. For analyses where the interaction between factors was significant, post-hoc comparisons were conducted across all group means. If no significant interaction effect was detected, Tukey's HSD test was used to compare means across the three different levels of the factor that showed a significant main effect (either temperature or metal exposure). All statistical analyses were conducted using GraphPad Prism version 7.05 (GraphPad Software Inc.).

To visualize differences between experimental exposure groups based on the entire immune dataset, Partial Least Squares–Discriminant Analysis (PLS-DA) was conducted using MetaboAnalyst 6.0 [68]. PLS-DA is a supervised method that uses multivariate regression techniques to extract, via linear combinations of the original variables, the information that best predicts membership in experimental groups. To minimize bias arising from differences in absolute scale among variables, data were autoscaled by mean-centering and dividing by the standard deviation of each variable. The relationships between different immune variables were further examined using Pearson correlation analysis, as implemented in MetaboAnalyst 6.0. Statistical significance was set at $p < 0.05$.

3. Results

3.1. Metal concentrations in water and oyster tissues

The measured Zn concentrations in the exposure water were 23.3 ± 2.2, 43.4 ± 4.1, and 302.7 ± 14.8 μg L^{-1} (mean ± SEM, N = 30) for the control, ZnL, and ZnH exposures, respectively. Cu concentrations in the water are not reported due to technical issues arising from mass interferences and inconsistent isotopic signals during quantification.

Baseline concentrations of Cu and Zn in control oyster tissues were 73.0 ± 9.5 μg g^{-1} and 1240.5 ± 113.7 μg g^{-1}, respectively (N = 24). Acclimation temperature did not have a significant effect on baseline Cu or Zn concentrations in oysters maintained under control conditions ($p > 0.05$). At low metal exposures, tissue metal concentrations in oysters exposed to Cu and Zn were comparable to control levels (CuL: 74.1 ± 7.9 μg g^{-1} Cu; ZnL: 1453.2 ± 103.2 μg g^{-1} Zn; $N = 24$) and did not vary significantly with temperature ($p > 0.05$). At high exposure levels, however, metal accumulation became temperature dependent ($p < 0.05$). In the CuH treatment, tissue Cu concentrations were 104.4 ± 12.4, 306.6 ± 61.8, and 381.9 ± 78.6 μg g^{-1} at 5, 15, and 22 °C, respectively ($N = 7–8$). In the ZnH treatment, tissue Zn concentrations were 1404.5 ± 89.9, 3152.6 ± 439.4, and 4573.6 ± 603.8 μg g^{-1} at 5, 15, and 22 °C, respectively ($N = 8$).

3.2. Combined effects of temperature and Zn exposure on immune parameters

In the combined temperature and Zn exposure experiments, significant temperature × Zn exposure interactions ($p < 0.05$, η^2 = 9–13 %) were observed for nitric oxide (NO) levels in hemocytes, as well as for phenoloxidase (PhO) and lysozyme (LYZ) activities in the hemolymph of juvenile oysters, indicating that the impact of Zn on these immune parameters was modulated by the acclimation temperature (Table 2). Furthermore, acclimation temperature had significant effects ($p < 0.05$) on hemocyte count, phagocytosis rate, lipid peroxidation (LPO) levels, and acid phosphatase (AP) activity in hemocytes accounting for 32–58 % of variation in these traits (Table 2). Zn exposure concentration had a significant effect on phagocytosis rate and AP activity ($p < 0.05$; η^2 = 10–19 %) (Table 2).

Hemocyte abundance was strongly affected by acclimation temperature ($p < 0.05$, η^2 = 48.2 %; Table 2) and was highest at 15 °C compared to both 5 °C and 22 °C (Fig. 2A). Zn exposure did not affect hemocyte abundance, regardless of the exposure temperature ($p > 0.05$; Table 2, Fig. 2A).

Phagocytosis rates were affected by both temperature and Zn exposure ($p < 0.05$; Table 2) and increased with rising Zn exposure concentrations across all temperature conditions (Fig. 2B). Phagocytosis

Table 2
ANOVA Results: Effects of temperature, exposure to different Zn concentrations, and their interactions on immune parameters in oyster juveniles
F-values with degrees of freedom for the effect and the error (in brackets), P-values, and effect sizes (η^2 = % variance explained) for factors and their interactions are provided. Significant effects are highlighted in bold. Abbreviations: HC – hemocytes, LPO – lipid peroxidation levels measured as concentration of thiobarbituric-acid reactive substances (TBARS), NO – nitric oxide.

Parameter	Temperature	Zn exposure	Interaction
HC count	**F (2, 45) = 22.34**	F (2, 45) = 0.57	F (4, 45) = 0.48
	P < 0.0001	P = 0.5673	P = 0.7495
	η^2 = 48.2 %	η^2 = 1.2 %	η^2 = 2.1 %
Phagocytosis rate	**F (2, 45) = 16.35**	**F (2, 45) = 9.36**	F (4, 45) = 1.09
	P < 0.0001	**P = 0.0004**	P = 0.3727
	η^2 = 32.4 %	η^2 = 18.6 %	η^2 = 4.3 %
LPO levels	**F (2, 45) = 36.25**	F (2, 45) = 0.99	F (4, 45) = 1.41
	P < 0.0001	P = 0.3779	P = 0.2449
	η^2 = 57.9 %	η^2 = 1.6 %	η^2 = 4.5 %
NO levels	**F (2, 45) = 59.92**	**F (2, 45) = 10.81**	**F (4, 45) = 6.70**
	P < 0.0001	**P = 0.0001**	**P = 0.0003**
	η^2 = 56.2 %	η^2 = 10.1 %	η^2 = 12.6 %
Acid phosphatase activity	**F (2, 45) = 51.80**	**F (2, 45) = 8.09**	F (4, 45) = 0.82
	P < 0.0001	**P = 0.0010**	P = 0.5183
	η^2 = 61.6 %	η^2 = 9.6 %	η^2 = 2.0 %
Phenoloxidase activity	**F (2, 45) = 19.84**	**F (2, 45) = 57.00**	**F (4, 45) = 5.13**
	P < 0.0001	**P < 0.0001**	**P = 0.0017**
	η^2 = 18.1 %	η^2 = 52.0 %	η^2 = 9.4 %
Lysozyme activity	**F (2, 45) = 14.06**	**F (2, 45) = 3.63**	**F (4, 45) = 2.82**
	P < 0.0001	**P = 0.0345**	**P = 0.0358**
	η^2 = 30.7 %	η^2 = 7.9 %	η^2 = 12.3 %

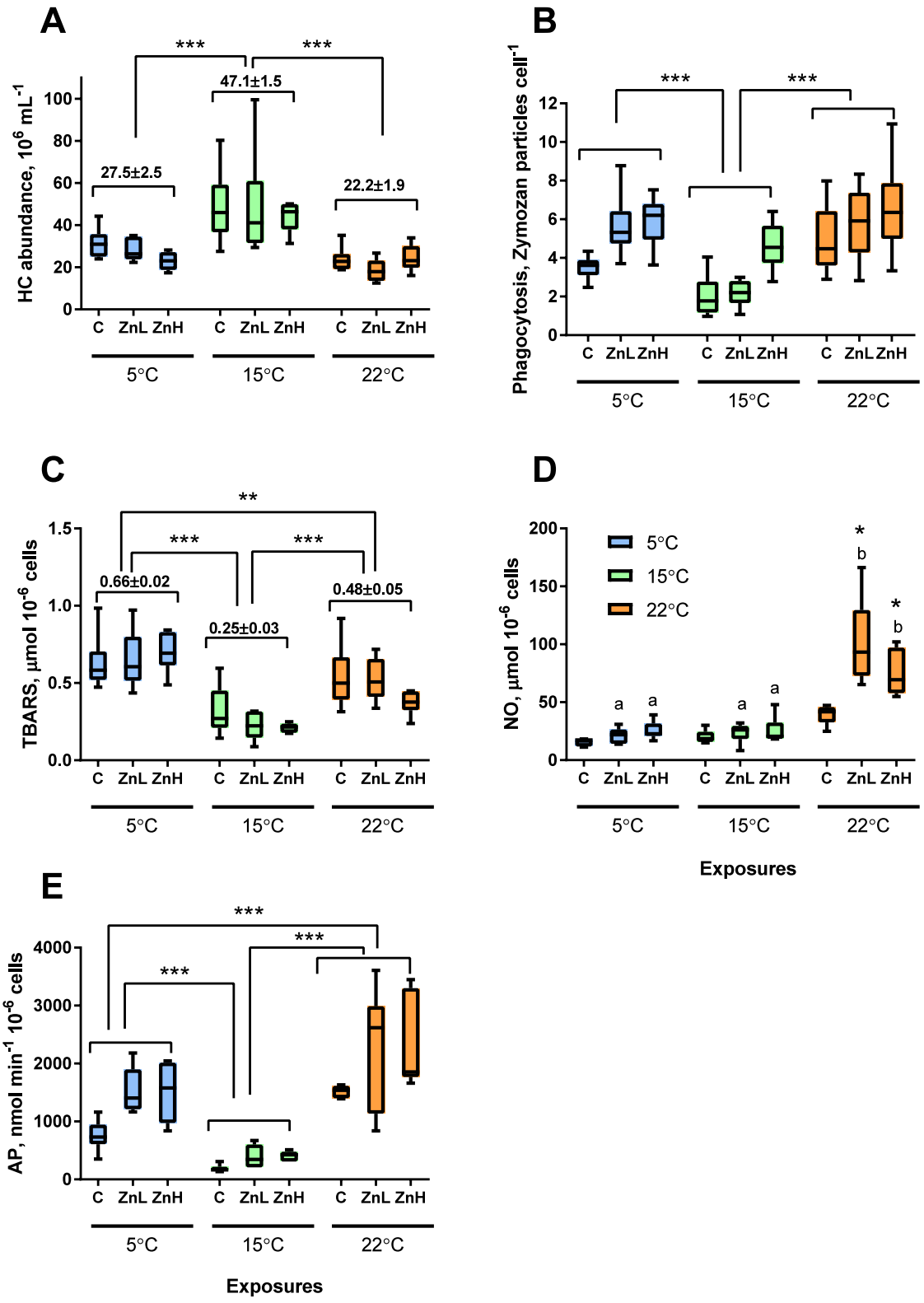

Fig. 2. Combined effects of temperature and Zn exposure on hemocyte immune parameters in juvenile oysters (*O. edulis*).
(A) hemocyte (HC) abundance, (B) phagocytosis rate, (C) lipid peroxidation (LPO) levels (TBARS), (D) nitric oxide (NO) levels, and (E) acid phosphatase (AP) activity. C - control, ZnL - low Zn concentration (nominal 100 µg L^{-1}), and ZnH - high Zn concentration (nominal 1000 µg L^{-1}). For HC abundance and LPO levels, where only significant temperature effects were observed, values above the brackets represent the temperature-specific mean ± SEM. Asterisks indicate significant differences between temperature exposure groups (*$p < 0.05$, **$p < 0.01$, *$p < 0.001$). For NO levels, where a significant interaction between temperature and Zn exposure was found, post-hoc comparisons of group means are shown: different letters indicate significant differences between temperature treatments within the same Zn exposure group, while asterisks indicate significant differences between Zn-exposed groups and their respective controls at the same temperature ($p < 0.05$). N = 6. (For interpretation of the references to color in this figure legend, the reader is referred to the legend in panel D in the Web version of this article.)

rates were lower at 15 °C than at either 5 °C or 22 °C (Fig. 2B).

LPO levels in hemocytes were strongly influenced by acclimation temperature ($p < 0.05$, $\eta^2 = 57.9$ %; Table 2), with the highest LPO levels observed in oysters acclimated to 5 °C and the lowest levels recorded at 15 °C (Fig. 2C). Zn exposure did not significantly influence LPO levels (Table 2, Fig. 2C).

Zn exposure significantly affected NO levels in hemocytes only at the highest acclimation temperature (22 °C), whereas no significant Zn-dependent variation in NO levels was detected at 5 °C or 15 °C (Fig. 2D). At 22 °C, NO levels in hemocytes from juvenile oysters exposed to low (ZnL) and high (ZnH) Zn concentrations were higher than in the temperature-matched control group or in oysters exposed to the same zinc concentrations at lower temperatures (5 °C and 15 °C) (Fig. 2D).

AP activity in hemocytes was significantly influenced by acclimation temperature ($p < 0.05$, $\eta^2 = 61.6$ %; Table 2), with the lowest AP activity observed in hemocytes of oysters acclimated to 15 °C and the highest levels recorded in those maintained at 22 °C (Fig. 2E). Zn exposure led to a significant increase in AP activity ($p < 0.05$, $\eta^2 = 9.6$ %; Table 2). AP activity in hemocytes was similar between oysters exposed to low and high Zn concentrations (Tukey's HSD, $p > 0.05$) and was significantly higher than in the control group ($p < 0.05$ for both ZnL and ZnH groups relative to the control) (Fig. 2E).

PhO activity in the hemolymph was significantly affected by Zn × temperature interactions ($p < 0.05$; Table 2). Generally, PhO activity decreased in a concentration-dependent manner with increasing Zn exposure concentrations across all acclimation temperatures (Table 2, Fig. 3A). In control oysters and those exposed to low Zn concentrations, hemocyte PhO activity was higher at 15 °C compared to both 5 °C and 22 °C. However, this temperature-dependent difference disappeared in hemocytes of ZnH group, reflecting strong PhO suppression by high Zn exposure concentration (Fig. 3A).

LYZ activity in the hemolymph was significantly affected by Zn × temperature interactions ($p < 0.05$; Table 2). In the control group, no difference in the hemolymph LYZ activity was found between the oysters acclimated at different temperatures (Fig. 3B). In both ZnL and ZnH groups, LYZ activity in the hemolymph was higher at 5 °C than at either 15 °C or 22 °C (Fig. 3B). Generally, Zn exposure had no significant effect on LYZ activity when compared to the temperature-matched controls ($p > 0.05$), except for the ZnL group at 5 °C that showed elevated LYZ activity compared to the control baseline (Fig. 3B).

3.3. Combined effects of temperature and Cu exposure on immune parameters

In the combined temperature and Cu exposure experiments, significant temperature × Cu exposure interactions ($p < 0.05$) were observed for LPO, NO levels and AP activity in hemocytes, as well as for PhO

Table 3
ANOVA Results: Effects of temperature, exposure to different Cu concentrations, and their interactions on immune parameters in oyster juveniles
F-values with degrees of freedom for the effect and the error (in brackets), P-values, and effect sizes (η^2 = % variance explained) for factors and their interactions are provided. Significant effects are highlighted in bold. Abbreviations: HC – hemocytes, LPO – lipid peroxidation levels measured as concentration of thiobarbituric-acid reactive substances (TBARS), NO – nitric oxide.

Parameter	Temperature	Cu exposure	Interaction
HC count	**F (2, 45) = 31.70**	F (2, 45) = 2.67	F (4, 45) = 0.36
	P < 0.0001	P = 0.0806	P = 0.8368
	η^2 = 55.1 %	η^2 = 4.6 %	η^2 = 1.3 %
HC mortality	**F (2, 45) = 11.21**	**F (2, 45) = 28.44**	F (4, 45) = 0.70
	P = 0.0001	**P < 0.0001**	P = 0.5986
	η^2 = 17.6 %	η^2 = 44.7 %	η^2 = 2.2 %
Phagocytosis rate	**F (2, 45) = 6.51**	F (2, 45) = 0.29	F (4, 45) = 2.35
	P = 0.0033	P = 0.7461	P = 0.0687
	η^2 = 19.1 %	η^2 = 0.9 %	η^2 = 13.8 %
LPO levels	**F (2, 45) = 5.18**	**F (2, 45) = 5.61**	**F (4, 45) = 5.81**
	P = 0.0095	**P = 0.0067**	**P = 0.0007**
	η^2 = 11.5 %	η^2 = 12.5 %	η^2 = 25.9 %
NO levels	**F (2, 45) = 62.97**	**F (2, 45) = 7.33**	**F (4, 45) = 5.13**
	P < 0.0001	**P = 0.0018**	**P = 0.0017**
	η^2 = 61.1 %	η^2 = 7.1 %	η^2 = 10.0 %
Acid phosphatase activity	**F (2, 44) = 31.80**	**F (2, 44) = 9.08**	**F (4, 44) = 2.89**
	P < 0.0001	**P = 0.0005**	**P = 0.0328**
	η^2 = 46.6 %	η^2 = 13.3 %	η^2 = 8.5 %
Phenoloxidase activity	F (2, 43) = 0.89	**F (2, 43) = 17.72**	**F (4, 43) = 11.27**
	P = 0.4174	**P < 0.0001**	**P < 0.0001**
	η^2 = 1.5 %	η^2 = 28.9 %	η^2 = 36.7 %
Lysozyme activity	**F (2, 44) = 21.97**	F (2, 44) = 2.27	F (4, 44) = 1.65
	P < 0.0001	P = 0.1154	P = 0.1780
	η^2 = 44.8 %	η^2 = 4.6 %	η^2 = 6.8 %

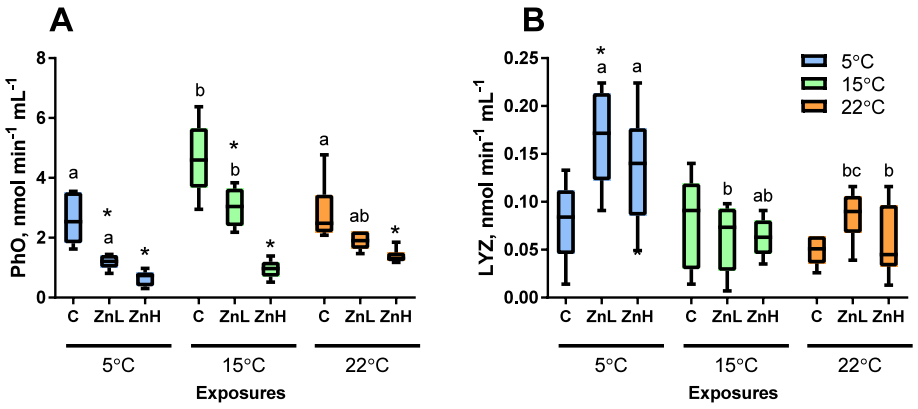

Fig. 3. Combined effects of temperature and Zn exposure on activity of immune enzymes in hemolymph of juvenile oysters (*O. edulis*).
(A) phenoloxidase (PhO) activity, (B) lysozyme (LYZ) activity. C - control, ZnL - low Zn concentration (nominal 100 μg L^{-1}), and ZnH - high Zn concentration (nominal 1000 μg L^{-1}). Due to a significant interaction between temperature and Zn exposure, only post-hoc comparisons of group means are shown: different letters indicate significant differences between temperature treatments within the same Zn exposure group, while asterisks indicate significant differences between Zn-exposed groups and their respective controls at the same temperature ($p < 0.05$). N = 6. (For interpretation of the references to color in this figure legend, the reader is referred to the panel B in the Web version of this article.)

activity in the hemolymph (Table 3). The significant interaction indicates that the effects of Cu exposure on these immune-related traits were modulated by acclimation temperature, thereby preventing the interpretation of single-factor effects. In contrast, hemocyte count, hemocyte mortality, phagocytosis rate, and LYZ activity showed no significant interaction effects of temperature × Cu exposure ($p > 0.05$). Acclimation temperature had significant effects ($p < 0.05$) on hemocyte count, hemocyte mortality, phagocytosis rate, and LYZ activity (Table 3), whereas Cu exposure concentration had a significant effect on hemocyte mortality ($p < 0.05$) (Table 3).

The hemocyte count showed a strong effect of temperature (effect size $\eta^2 = 55.1$ %; $p < 0.05$) but no effects of Cu exposure ($p > 0.05$) (Table 3). The average hemocyte count was comparable in juvenile oysters acclimated to 5 °C and 15 °C but significantly lower in those acclimated to 22 °C, regardless of Cu exposure (Fig. 4A).

The hemocyte mortality increased with both acclimation temperature and Cu exposure concentration, with these factors accounting for 17.6 % and 44.7 % of the observed data variation, respectively (Table 3). In general, the hemocyte mortality in control oysters was significantly lower than in both Cu-exposed groups (Tukey's HSD, $p < 0.05$) (Fig. 4B). No significant difference in the hemocyte mortality was observed between oysters exposed to low and high Cu concentrations ($p > 0.05$). Hemocyte mortality in juvenile oysters increased with increasing acclimation temperature (Fig. 4B).

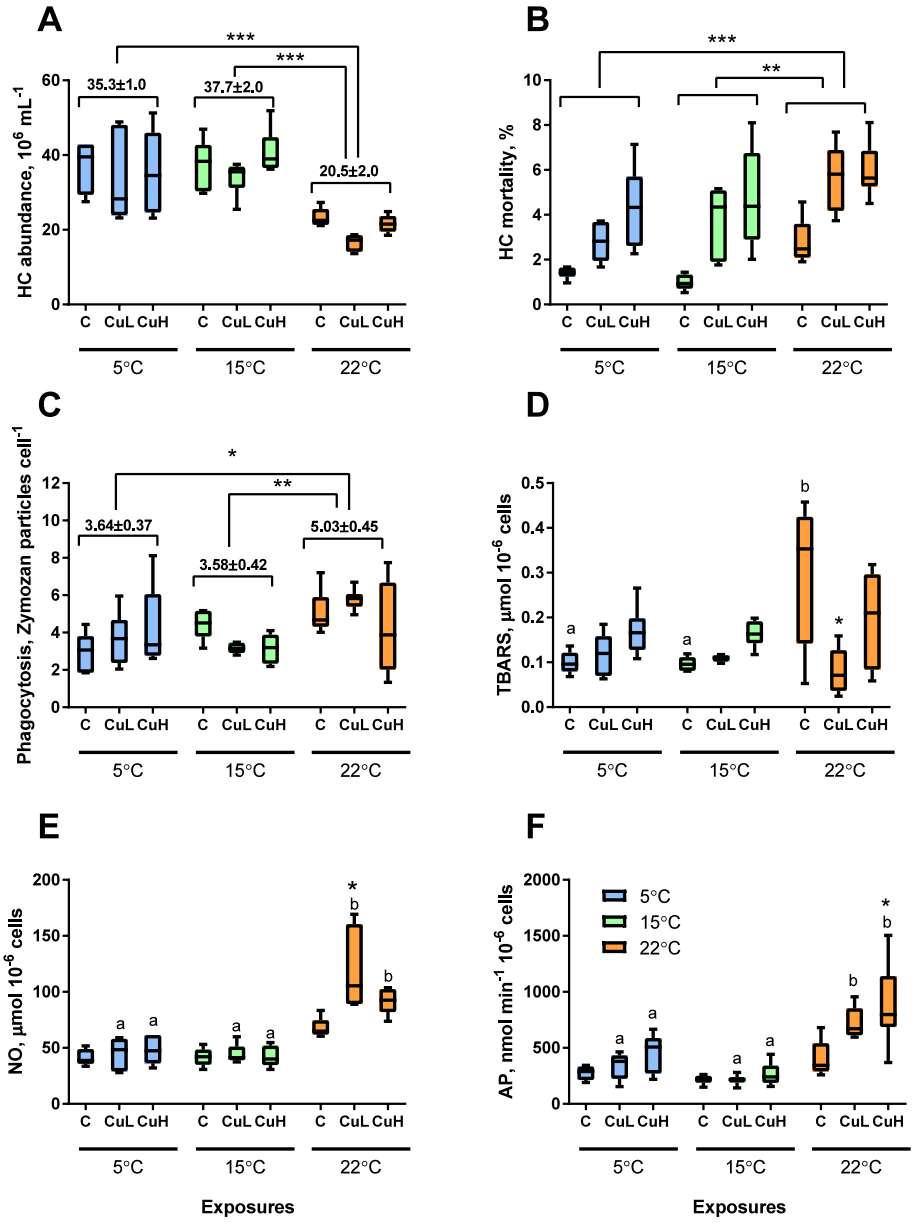

Fig. 4. Combined effects of temperature and Cu exposure on hemocyte immune parameters in juvenile oysters (*O. edulis*).
(A) hemocyte (HC) abundance, (B) phagocytosis rate, (C) lipid peroxidation (LPO) levels (TBARS), (D) nitric oxide (NO) levels, and (E) acid phosphatase (AP) activity. C - control, CuL - low Cu concentration (nominal 10 μg L^{-1}), and CuH - high Cu concentration (nominal 100 μg L^{-1}). For HC abundance and phagocytosis rates, where only significant temperature effects were observed, values above the brackets represent the temperature-specific mean ± SEM. Asterisks indicate significant differences between temperature exposure groups (*$p < 0.05$, **$p < 0.01$, *$p < 0.001$). For LPO, NO levels and AP activity, where a significant interaction between temperature and Cu exposure was found, post-hoc comparisons of group means are shown: different letters indicate significant differences between temperature treatments within the same Cu exposure group, while asterisks indicate significant differences between Cu-exposed groups and their respective controls at the same temperature ($p < 0.05$). N = 5–6. (For interpretation of the references to color in this figure legend, the reader is referred to the panel F in the Web version of this article.)

Hemocyte phagocytosis rates showed only significant effects of temperature ($p < 0.05$, $\eta^2 = 19.1$ %, Table 3). Phagocytosis rates were comparable in hemocytes of oysters acclimated to 5 °C and 15 °C but significantly elevated in those maintained at 22 °C (Fig. 4C). Cu exposure had no consistent effect on this parameter in juvenile oysters (Table 3, Fig. 4C).

LPO levels in hemocytes of juvenile *O. edulis* showed a significant interactive effect of temperature and Cu exposure (interaction effect size: 25.9 %, $p < 0.05$; Table 3). In control oysters, elevated temperature (22 °C) resulted in a significant increase in LPO levels (Fig. 4D). At lower temperatures (5 °C and 15 °C), there was a non-significant trend of increasing LPO levels with increasing Cu exposure concentrations; however, this trend was not observed at 22 °C, where the lowest LPO levels occurred in the CuL group (Fig. 4D).

NO levels in hemocytes showed temperature-dependent effects of Cu exposure (interaction effect size: 10 %, $p < 0.05$; Table 3). High temperature (22 °C) led to elevated NO levels in hemocytes, particularly when combined with Cu exposure (Fig. 4E). However, at 5 °C and 15 °C Cu exposure had no effect on NO levels in hemocytes of oysters (Fig. 4E).

A similar pattern was observed for AP activity in hemocytes, with a significant temperature-Cu interaction effect (interaction effect size: 8.5 %, $p < 0.05$; Table 3). Warming to 22 °C stimulated AP activity in oyster hemocytes, especially when combined with Cu exposure, whereas at 5 °C and 15 °C, Cu had no effect on AP activity (Fig. 4F).

PhO activity in oyster hemocytes showed temperature-dependent sensitivity to Cu exposure (interaction effect size: 36.7 %, $p < 0.05$; Table 3). Cu exposure resulted in elevated PhO activity at 5 °C (in both CuL and CuH groups) and at 15 °C (in the CuH group) relative to their respective controls. However, at 22 °C, no significant effects of Cu exposure were detected (Fig. 5A).

LYZ activity was strongly influenced by temperature (effect size: 44.8 %, $p < 0.05$; Table 3), with significantly lower LYZ activity observed in the hemolymph of oysters acclimated to 15 °C compared to those maintained at 5 °C and 22 °C. Cu exposure had no significant effect on LYZ activity, regardless of temperature (Fig. 5B).

3.4. Multivariate analysis of immune biomarker data

PLS-DA analysis revealed a clear separation of immune parameter profiles between different temperature acclimation groups in both the temperature-Zn and temperature-Cu exposure experiments, as shown in the plane of the first two principal components (Fig. 6).

In the Zn exposure experiment, the immune profile of juvenile oysters acclimated to 22 °C was separated along PC1 (which explained 29.9 % of data variation) from those acclimated to 5 °C or 15 °C. PC1 exhibited high positive loadings (>0.3) for phagocytosis rates, NO levels, and AP activity, while total hemocyte count had a high negative loading (<-0.3) (Supplementary Table 1; Fig. 6A). The immune profiles of oysters acclimated to 5 °C and 15 °C were separated along PC2, which had high positive loadings for hemocyte count and PhO activity and high negative loadings for phagocytosis rate, LPO levels, AP activity, and LYZ activity (Supplementary Table 1). The immune profiles of control and Zn-exposed oysters were separated along PC1 in the 22°C-acclimated group, whereas in the 5 °C and 15 °C groups, separation occurred along PC2 (Fig. 6A).

In the Cu exposure experiment, oysters acclimated to 22 °C exhibited a shift along PC1 (explaining 42 % of data variation), while those acclimated to 5 °C and 15 °C were separated from each other along PC2 (12.3 % variation) (Fig. 6B). PC1 had high positive loadings (>0.3) for hemocyte mortality, phagocytosis rates, NO levels, and AP activity, whereas total hemocyte count had a high negative loading (<-0.3) (Supplementary Table 2; Fig. 6B). Similar to the Zn exposure experiment, the immune profiles of oysters acclimated to 5 °C and 15 °C were separated along PC2, which had high negative loadings for PhO and LYZ activity (Supplementary Table 2). The immune profiles of control and Cu-exposed oysters were separated along PC1 in the 22°C-acclimated group and along PC2 in the 5 °C and 15 °C groups (Fig. 6B). However, compared to the Zn exposure experiment, the Cu-exposed groups exhibited greater overlap (Fig. 6B).

Hemocyte abundance in juvenile oysters was negatively correlated with phagocytosis activity (Pearson correlation coefficient $r = -0.54$ to -0.66), NO levels ($r = -0.52$ to -0.83), and AP activity ($r = -0.63$ to -0.64) in both experimental datasets from temperature–Zn and temperature–Cu exposures. Furthermore, in the temperature–Cu experiment, hemocyte count was negatively correlated with hemocyte mortality ($r = -0.54$), and hemocyte mortality was positively correlated with NO levels ($r = 0.60$) and AP activity ($r = 0.57$). Data on hemocyte mortality were not available for the Zn exposure experiment. Additionally, phagocytosis rates were positively associated with NO levels ($r = 0.41$ to 0.54) and AP activity ($r = 0.55$ to 0.76) in hemocytes across both experiments. Other immune parameters exhibited either weak ($r < 0.4$) correlations or inconsistent correlation patterns across the two

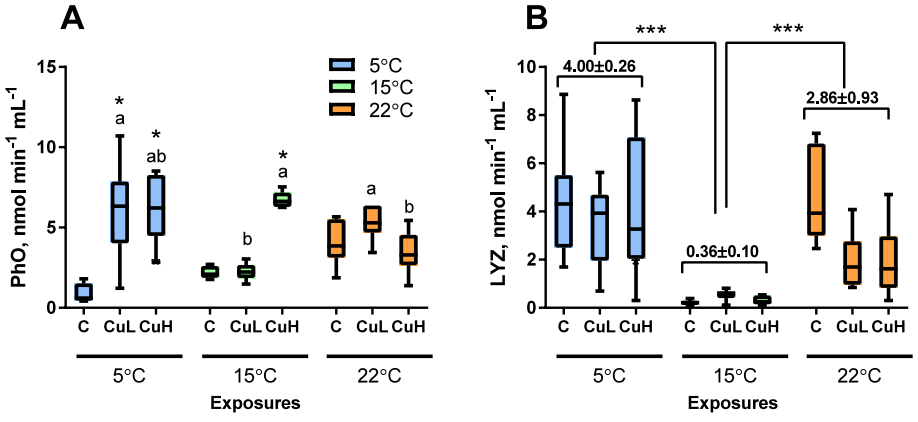

Fig. 5. Combined effects of temperature and Cu exposure on hemocyte immune parameters in juvenile oysters (*O. edulis*).
(A) phenoloxidase (PhO) activity, (B) lysozyme (LYZ) activity. C - control, CuL - low Cu concentration (nominal 10 μg L^{-1}), and CuH - high Cu concentration (nominal 100 μg L^{-1}). Asterisks indicate significant differences between temperature exposure groups for LYZ activity where no significant interaction with Cu exposure was detected (*$p < 0.05$, **$p < 0.01$, *$p < 0.001$). Values above brackets show temperature-specific mean ± SEM. For PhO activity, where a significant interaction between temperature and Cu exposure was found, post-hoc comparisons of group means are shown: different letters indicate significant differences between temperature treatments within the same Cu exposure group, while asterisks indicate significant differences between Cu-exposed groups and their respective controls at the same temperature ($p < 0.05$). N = 5–6. (For interpretation of the references to color in this figure legend, the reader is referred to the panel A in the Web version of this article.)

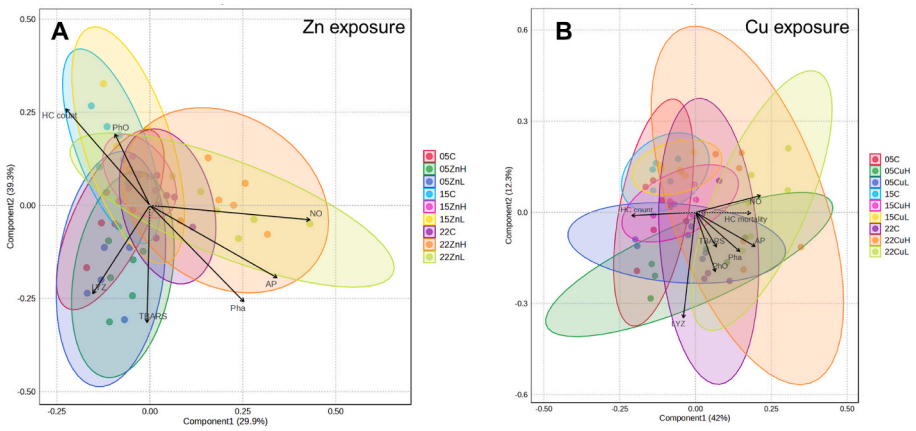

Fig. 6. Biplot of the immune profiles of *O. edulis* juveniles exposed to different temperatures and Zn (A) or Cu (B) concentrations.
Data from individual samples are plotted in the plane of the first two PLS-DA components. Different exposure groups are distinguished by color, and shaded ovals represent the 95 % confidence interval. Exposure groups: 05C – control at 5 °C; 15C – control at 15 °C; 22C – control at 22 °C; 05ZnH – high Zn concentration (nominal 1000 μg L^{-1}) at 5 °C; 05ZnL – low Zn concentration (nominal 100 μg L^{-1}) at 5 °C; 15ZnH – high Zn concentration (nominal 1000 μg L^{-1}) at 15 °C; 15ZnL – low Zn concentration (nominal 100 μg L^{-1}) at 15 °C; 22ZnH – high Zn concentration (nominal 1000 μg L^{-1}) at 22 °C; 22ZnL – low Zn concentration (nominal 100 μg L^{-1}) at 22 °C; 05CuH – high Cu concentration (nominal 100 μg L^{-1}) at 5 °C; 05CuL – low Zn concentration (nominal 10 μg L^{-1}) at 5 °C; 15CuH – high Cu concentration (nominal 100 μg L^{-1}) at 15 °C; 15CuL – low Cu concentration (nominal 10 μg L^{-1}) at 15 °C; 22CuH – high Cu concentration (nominal 100 μg L^{-1}) at 22 °C; 22CuL – low Cu concentration (nominal 10 μg L^{-1}) at 22 °C. Abbreviations of the immune parameters: HC – hemocytes; TBARS – lipid peroxidation (LPO) levels measured as TBARS; Pha – phagocytosis rates; NO – nitric oxide levels; LYZ – lysozyme activity; AP – acid phosphatase activity; PhO – phenoloxidase activity. (For interpretation of the references to color in this figure legend, the reader is referred to the Web version of this article.)

experiments (Supplementary Table 2).

4. Discussion

Our study revealed complex interactions between temperature and trace metal exposure on the cellular and humoral immune responses of juvenile *O. edulis*. PhO activity and hemocyte NO levels showed consistent interactive effects of temperature and metal exposure in both Zn and Cu experiments, indicating that the influence of Zn and Cu on these immune parameters depended on acclimation temperature. Notably, for most of the studied immune traits, environmental temperature emerged as the dominant immunomodulatory factor, explaining a large proportion of the observed variance. The only exceptions were hemocyte mortality, which was strongly affected by Cu exposure (~45 % of variation), and PhO activity, which showed substantial effects of both Zn and Cu exposure (~52 % and ~29 % of variation, respectively). The strong influence of temperature on *O. edulis* immunity was further supported by PLS-DA analysis, which showed clearer separation of immune profiles by temperature than by metal exposure. This pattern aligns with previous findings in other ectotherms, including bivalves, showing pronounced effects of temperature on innate immunity [33, 69–71].

The baseline (control) concentrations of Zn and Cu in juvenile oysters in the present study (1240.5 ± 113.7 μg g^{-1} and 73.0 ± 9.5 μg g^{-1} dry mass, respectively) fall within the range typically reported for oysters from unpolluted environments [72–76]. This is consistent with the origin of our experimental oysters from a hatchery producing spat for aquaculture and exposed to minimal anthropogenic contamination. Both Zn and Cu are essential trace elements [77–80], and relatively high tissue concentrations are normal and expected in healthy oysters. As commonly observed in oysters, Zn concentrations were considerably higher than those of Cu [72–76,81]. This pattern is also characteristic of *O. edulis*. For example, *O. edulis* collected from Restronguet Creek in the Fal Estuary (UK) contained Cu concentrations ranging from 40 to 16, 500 μg g^{-1} and Zn concentrations from 1500 to 11,710 μg g^{-1} dry mass [82]. No accumulation of Zn or Cu was observed in *O. edulis* juveniles exposed to low test concentrations (100 μg L^{-1} Zn or 10 μg L^{-1} Cu), indicating efficient regulation of tissue levels of these essential metals. In contrast, at higher exposures (1000 μg L^{-1} Zn or 100 μg L^{-1} Cu), significant metal accumulation occurred in oyster tissues, and this effect was further enhanced at elevated temperatures. In aquatic organisms, increased metal accumulation at higher temperatures is commonly observed and is often attributed to a higher temperature-dependence (Q_{10}) for metal uptake relative to metal elimination [35].

Temperature is a key environmental factor influencing all aspects of oyster metabolism and physiology, as it directly affects the rates of biochemical and physiological processes in ectothermic organisms [83]. The temperature optimum for *O. edulis* survival and growth varies between populations and life stages. In larvae, temperatures between 12.5° and 27.5 °C allowed good survival, whereas survival was poor at 10 °C and 30 °C [84]. For spat, the optimum temperature for settlement was 20–22.5 °C, with growth increasing between 12.5° and 27.5 °C, and no growth observed at 10 °C [84]. In adults, the optimal temperature range for growth, as determined by scope-for-growth measurements, was 15–25 °C [85–87]. Accordingly, the lower test temperature in our study (5 °C) falls below the thermal optimum for *O. edulis*, whereas the other two experimental temperatures (15 °C and 22 °C) are within the optimal range for both juveniles and adults.

We observed a strong effect of temperature on most cellular immunity parameters in juvenile *O. edulis*. Temperature accounted for nearly 50 % of the variation in hemocyte abundance, whereas exposure to Zn and Cu had no significant effect, explaining less than 5 % of the observed variability. Hemocyte counts were highest at the intermediate temperature of 15 °C, while exposure to 5 °C (in the Zn experiment) and 22 °C (in both Zn and Cu experiments) led to a decline. Circulating hemocyte count is a dynamic parameter influenced by hematopoiesis, hemocyte mortality, and tissue migration [88]. In *O. edulis* juveniles, temperature had only a modest effect on hemocyte mortality (2.8 % at 22 °C vs. 1.0–1.4 % at 5 °C and 15 °C), indicating that temperature-related variation in hemocyte count likely reflects other processes such as increased hematopoiesis or tissue mobilization. Similarly, studies on the Pacific oyster *Crassostrea gigas* show high thermal tolerance of hemocytes, with significant mortality only above 35 °C [69] and peak circulating counts around 25 °C [89]. These temperature-dependent shifts are likely multifactorial: elevated temperatures may transiently mobilize hemocytes as part of a general stress response, while prolonged warming can increase metabolic demand and divert resources from immune maintenance. Conversely, low temperatures suppress metabolism and

hematopoiesis, reducing circulating cell numbers [90,91]. The highest hemocyte abundance observed at 15 °C in *O. edulis* suggests this temperature may represent an immunological "sweet spot" for immune surveillance of this species.

Phagocytosis is a key mechanism of pathogen removal in the bivalve immune system [10,88]. The phagocytosed pathogens are destroyed by lysosomes upon the fusion of the phagosome with them, and acid phosphatase (AP) activity plays a key role in this process [10]. AP is a lysosomal hydrolase that catalyzes the dephosphorylation of a wide variety of substrates, including proteins, lipids, and nucleic acids, at acidic pH [92,93]. It contributes directly to the intracellular digestion and killing of phagocytosed microbes [92]. In immune cells, high AP activity is a hallmark of phagolysosomes, where it aids in the degradation of pathogen components and helps regulate signaling by dephosphorylating both microbial and host molecules. This supports both microbicidal activity and the regulation of inflammatory responses [92–95]. Our study demonstrated elevated phagocytic activity in hemocytes of juveniles acclimated to 22 °C compared to those maintained at an intermediate temperature of 15 °C, suggesting that mild warming (within the optimum range of *O. edulis*) can stimulate cellular clearance mechanisms. Immunostimulatory effects of warming have been reported in other bivalves. For example, studies on *C. gigas* have shown that mortality from outbreaks of *Ostreid herpesvirus 1* (OsHV-1) was significantly reduced when temperatures exceed 24 °C [96]. This protective effect was associated with the transcriptional upregulation of innate immunity and apoptosis, which help eliminate pathogens and virus-infected host cells [96]. Additionally, warming to 22 °C enhanced the expression of numerous immune-related genes in *C. gigas* adults and juveniles injected with a viral antigen [70]. However, while adults showed a delayed immune response (26 h post-injection) and good survival, juveniles responded earlier (12 h post-injection) with a strong immune reaction that led to immune-mediated disorders and increased mortality [70]. These findings indicate that moderate warming can enhance immune activation in bivalves; however, the effects appear to vary across developmental stages, likely reflecting a balance between protective and potentially deleterious immune responses. Interestingly, exposure to cold conditions outside the optimal thermal range of *O. edulis* (5 °C) also resulted in elevated phagocytosis rates in hemocytes, albeit this trend was only significant in the Zn exposure experiment. The mechanisms underlying this cold-induced immune activation remain unclear, but it may be associated with increased tissue damage at low temperatures, which could in turn stimulate immune responses.

Metal-induced effects on cellular immune parameters of juvenile *O. edulis* were generally weaker than those induced by temperature within the tested range. Thus, Cu exposure significantly increased hemocyte mortality in juvenile *O. edulis*, consistent with the known cytotoxic effects of this metal [29,30,58]. However, this did not translate into a reduction in overall hemocyte abundance, suggesting that hemocyte loss due to metal-induced cell death can be compensated through hematopoiesis or the recruitment of hemocytes from tissues. Furthermore, Cu exposure had no notable effect on phagocytosis in *O. edulis*, although it stimulated AP activity, most notably at 22 °C. In other bivalves, impact of Cu on cellular immunity differs depending on species and Cu concentration. For instance, in freshwater mussels (*Diplodon chilensis*), dietary exposure to Cu-enriched algae enhanced both phagocytic and AP activity [97]. In marine species, lower Cu concentrations (200 μg L^{-1}) stimulated phagocytosis in *M. edulis*, while higher levels (500 μg L^{-1}) were suppressive [98]. In contrast, phagocytosis was inhibited in *Mytilus galloprovincialis* and *Ruditapes philippinarum* exposed to 0.5–1 μM Cu (32–64 μg L^{-1}) [99], and in *Perna viridis* at 50–200 μg L^{-1} [100]. Moreover, both dissolved Cu (20–50 μg L^{-1} $CuSO_4$) and nano-CuO (100–450 μg L^{-1}) suppressed phagocytosis in *M. galloprovincialis* [101]. Unlike Cu, exposure to Zn consistently stimulated both phagocytosis and acid phosphatase (AP) activity across all tested temperatures in *O. edulis*. Similar upregulation of phagocytic activity has been reported in hemocytes of *M. edulis* exposed to nano-ZnO or ionic Zn (10–100 μg L^{-1}) [24,32,33], consistent with the well-established role of zinc as an immunostimulant [102,103].

We also observed temperature- and metal-induced alterations in oxidative damage, measured as lipid peroxidation (LPO), and in the levels of the signaling molecule nitric oxide (NO) in hemocytes of *O. edulis* juveniles. Exposure to both 5 °C and 22 °C led to a significant increase in LPO compared to the intermediate temperature of 15 °C, indicating elevated oxidative stress. While the exact mechanisms remain unclear, the increase in LPO at elevated temperature of 22 °C may be attributed to enhanced metabolic activity and increased production of reactive oxygen species (ROS), whereas in the cold, oxidative damage could result from impaired antioxidant defenses, such as reduced enzymatic activity or glutathione availability [104–106]. In parallel, intracellular NO levels were elevated under warming (22 °C), particularly when combined with metal exposure. Elevated NO can contribute to cytotoxicity, mitochondrial dysfunction, and modulation of phagocytic signaling, potentially influencing overall immune competence [107–109]. The absence of immunoinhibition in *O. edulis* juveniles at elevated temperatures and metal exposures, despite increased NO levels, suggests that the observed NO elevation primarily serves a signaling role rather than inducing nitrosative stress or cytotoxicity.

In contrast to cellular immune parameters, which were primarily influenced by temperature, the humoral factors measured in hemolymph plasma of juvenile *O. edulis*—PhO and LYZ—exhibited distinct responses dependent on both temperature and metal exposure. PhO activity was particularly sensitive to Zn, showing a clear concentration-dependent decrease across all tested temperatures. The suppression of PhO activity by Zn suggests a potential weakening of humoral immune defenses under Zn stress, which may be partially alleviated by warming within the species' optimal temperature range [110]. In contrast, Cu exhibited no or slightly stimulatory effects on the studied humoral effectors: hemocyte PhO activity increased in Cu-exposed oysters at 5 °C and 15 °C, but remained unchanged at 22 °C, whereas LYZ activity did not respond to Cu exposure. By contrast, temperature had modest effects on PhO, producing a temperature-dependent increase that peaked at 15 °C in the Zn exposure experiment and at 22 °C in the Cu exposure experiment. Interestingly, LYZ activity in oyster hemolymph was stimulated by cold exposure (5 °C) indicating enhanced antibacterial capacity at low temperatures [111,112], potentially helping to maintain immune protection when other components of the immune system are temperature constrained. Overall, these findings highlight the complex interplay between temperature and metal exposure in shaping humoral immune responses, suggesting that environmental stressors may differentially modulate cellular and humoral defenses and, consequently, influence the host's overall immune defense.

4.1. Outlook and limitations

Our findings demonstrate that temperature is a strong immunomodulatory factor in *O. edulis* juveniles. In contrast, Zn and Cu at environmentally realistic concentrations had only minor effects on cellular and humoral immune markers, except for Zn-mediated suppression of PhO and Cu-induced hemocyte mortality, indicating a relatively low immunotoxic risk under typical field conditions. Given the bactericidal and parasiticidal properties of these metals, particularly Cu [58,59,113], low-level exposure may even indirectly support host defense by reducing pathogen pressure, although such effects are species-, life stage-, and context-dependent.

These findings have practical implications for aquaculture. Embryonic development remains highly sensitive to metal exposure, whereas larvae are generally more resilient, and low Cu concentrations may promote settlement [114,115]. Carry-over effects from larval metal exposure, however, can reduce spat growth (Noetzel, unpublished data), making metal-free hatchery conditions the most reliable strategy for early development. Juveniles past this developmental bottleneck appear resilient to low-level metal exposure under thermally optimal

conditions. Deploying seed in moderately contaminated but thermally suitable areas (summer maxima below ~22 °C) is unlikely to pose major immunological risks. Yet cold snaps (~5 °C) and heatwaves (>22 °C) could impair cell-based immune responses via reduced hemocyte abundance, oxidative stress, and altered immune enzyme activity, increasing pathogen susceptibility [92,116]. With marine heatwaves becoming more frequent, moderate warming benefits may quickly shift toward immune dysregulation and higher mortality risk [16,21]. Management should therefore prioritize careful site selection, avoid thermal extremes, and monitor immune biomarkers in hatchery stocks to guide release timing.

Important limitations remain. Our study covered a relatively narrow temperature range and did not explore thermal extremes, such as those expected during marine heatwaves. Only immunocompetence was assessed; experimental and field infection studies are needed to determine whether observed immune changes affect disease susceptibility. The effects of metal mixtures and complex pollutant cocktails are also poorly understood. Future research should identify thermal thresholds for immune impairment, explore multi-stressor interactions, and characterize thermally resilient oyster strains to support sustainable aquaculture under changing ocean conditions.

CRediT authorship contribution statement

Halina Falfushynska: Conceptualization, Methodology, Investigation, Funding acquisition, Formal analysis, Data curation, Writing – review & editing; **Dominique C. Noetzel**: Writing – review & editing, Investigation, Conceptualization; **Bernd Sures**: Methodology, Resources, Writing – review & editing; Milen Nachev: Methodology, Investigation, Validation, Writing – review & editing; **Bernadette Pogoda**: Writing – review & editing, Resources, Project administration, Funding acquisition, Conceptualization; **Bérenger Colsoul**: Resources, Writing – review & editing. **Inna M. Sokolova**: Writing – Original Draft Preparation, Writing – review & editing, Resources, Project administration, Methodology, Supervision, Supervision, Formal Analysis, Funding acquisition, Conceptualization.

Funding information

This work was funded by the German Federal Ministry of Education and Research (BMBF, award numbers 03F0836A and 03F0910D) within the framework CREATE (Concepts for Reducing the Effects of Anthropogenic pressures and uses on marine Ecosystems and on Biodiversity) as part of the mission SustainMare within the German Marine Research Alliance (DAM) to IMS And BP, and by the Philipp Schwartz Initiative of the Alexander von Humboldt Foundation (Germany) to HF. The views expressed in this publication are those of the authors and do not necessarily reflect the opinions or policies of the funding agencies.

Declaration of competing interest

The authors declare the following financial interests/personal relationships which may be considered as potential competing interests: Inna Sokolova was recently involved in preparing a report for the International Council on Mining and Metals (ICMM) Metals Environmental Risk Assessment Guidance (MERAG), entitled *"Environmental Risk Assessment of Metals: Guidance Review and Recommendations to Account for a Changing Climate,"* funded by the International Zinc Association (IZA). However, no financial support from ICMM or IZA was provided for the work described in the current manuscript, and their funding had no influence on the study's design, execution, or findings.

Appendix A. Supplementary data

Supplementary data to this article can be found online at https://doi.org/10.1016/j.fsi.2026.111119.

Data availability

Data will be made available on request.

References

[1] C.C. Vaughn, T.J. Hoellein, Bivalve impacts in freshwater and Marine ecosystems, Annu. Rev. Ecol. Evol. Syst. 49 (2018) 183–208.
[2] H.M. Jansen, Ø. Strand, W. van Broekhoven, T. Strohmeier, M.C. Verdegem, A. C. Smaal, Feedbacks from filter feeders: review on the role of mussels in cycling and storage of nutrients in Oligo- Meso- and eutrophic cultivation areas, in: A. C. Smaal, J.G. Ferreira, J. Grant, J.K. Petersen, Ø. Strand (Eds.), Goods and Services of Marine Bivalves, Springer International Publishing, Cham, 2019, pp. 143–177.
[3] S. Hynes, R. Burger, J. Tudella, D. Norton, W. Chen, Estimating the costs and benefits of protecting a coastal amenity from climate change-related hazards: nature based solutions via oyster reef restoration versus grey infrastructure, Ecol. Econ. 194 (2022) 107349.
[4] J.M. Guinotte, V.J. Fabry, Ocean acidification and its potential effects on marine ecosystems, Ann. N. Y. Acad. Sci. 1134 (2008) 320–342.
[5] B.R. Dumbauld, J.L. Ruesink, S.S. Rumrill, The ecological role of bivalve shellfish aquaculture in the estuarine environment: a review with application to oyster and clam culture in West Coast (USA) estuaries, Aquaculture 290 (2009).
[6] D.F. Willer, D.C. Aldridge, Sustainable bivalve farming can deliver food security in the tropics, Nat. Food 1 (2020) 384–388.
[7] A. Zgouridou, E. Tripidaki, I.A. Giantsis, J.A. Theodorou, M. Kalaitzidou, D. E. Raitsos, et al., The current situation and potential effects of climate change on the microbial load of marine bivalves of the Greek coastlines: an integrative review, Environ. Microbiol. 24 (2022) 1012–1034.
[8] A. Saco, B. Novoa, S. Greco, M. Gerdol, A. Figueras, Bivalves present the largest and Most diversified repertoire of toll-like receptors in the animal kingdom, suggesting broad-spectrum pathogen recognition in marine waters, Mol. Biol. Evol. 40 (2023).
[9] B. Allam, D. Raftos, Immune responses to infectious diseases in bivalves, J. Invertebr. Pathol. 131 (2015) 121–136.
[10] N.R. de la Ballina, F. Maresca, A. Cao, A. Villalba, Bivalve haemocyte subpopulations: a review, Front. Immunol. 13 (2022) 826255.
[11] S. De La Forest Divonne, J. Pouzadoux, O. Romatif, C. Montagnani, G. Mitta, D. Destoumieux-Garzón, et al., Diversity and functional specialization of oyster immune cells uncovered by integrative single-cell level investigations, eLife 13 (2025).
[12] A.V. Ivanina, H.I. Falfushynska, E. Beniash, H. Piontkivska, I.M. Sokolova, Biomineralization-related specialization of hemocytes and mantle tissues of the Pacific oyster *Crassostrea gigas*, J. Exp. Biol. 220 (2017) 3209–3221.
[13] V. Matozzo, A. Chinellato, M. Munari, L. Finos, M. Bressan, M.G. Marin, First evidence of immunomodulation in bivalves under seawater acidification and increased temperature, PLoS One 7 (2012) e33820.
[14] V. Matozzo, M.G. Marin, Bivalve immune responses and climate changes: is there a relationship? ISJ 8 (2011) 70–77.
[15] C.A. Burge, C. Mark Eakin, C.S. Friedman, B. Froelich, P.K. Hershberger, E. E. Hofmann, et al., Climate change influences on marine infectious diseases: implications for management and society, Ann. Rev. Mar. Sci 6 (2014) 249–277.
[16] F. Masanja, K. Yang, Y. Xu, G. He, X. Liu, X. Xu, et al., Impacts of marine heat extremes on bivalves, Front. Mar. Sci. 10 (2023).
[17] C. Gestal, P. Roch, T. Renault, A. Pallavicini, C. Paillard, B. Novoa, et al., Study of diseases and the immune system of bivalves using molecular biology and genomics, Fish. Sci. 16 (2008) 133–156.
[18] B. Allam, E. Pales Espinosa, Bivalve immunity and response to infections: are we looking at the right place? Fish Shellfish Immunol. 53 (2016) 4–12.
[19] T. Balbi, M. Auguste, C. Ciacci, L. Canesi, Immunological responses of marine bivalves to contaminant exposure: contribution of the -Omics approach, Front. Immunol. 12 (2021).
[20] M.A. Rahman, S. Henderson, P. Miller-Ezzy, X.X. Li, J.G. Qin, Immune response to temperature stress in three bivalve species: pacific oyster Crassostrea gigas, mediterranean mussel Mytilus galloprovincialis and mud cockle Katelysia rhytiphora, Fish Shellfish Immunol. 86 (2019) 868–874.
[21] F. Masanja, Y. Xu, K. Yang, R. Mkuye, Y. Deng, L. Zhao, Surviving the cold: a review of the effects of cold spells on bivalves and mitigation measures, Front. Mar. Sci. (2023). Volume 10 - 2023.
[22] A.V. Ivanina, C. Hawkins, I.M. Sokolova, Interactive effects of copper exposure and environmental hypercapnia on immune functions of marine bivalves *Crassostrea virginica* and *Mercenaria mercenaria*, Fish Shellfish Immunol. 49 (2016) 54–65.
[23] H. Falfushynska, O. Dellwig, A. Köhler, I.M. Sokolova, Adverse outcome pathways as a tool for optimization of the biomarker-based assessment of pollutant toxicity: a case study of cadmium in the blue mussels *Mytilus edulis*, Ecol. Indic. 158 (2024) 111431.
[24] F. Wu, H. Kong, L. Xie, I.M. Sokolova, Exposure to nanopollutants (nZnO) enhances the negative effects of hypoxia and delays recovery of the mussels' immune system, Environ. Pollut. 351 (2024) 124112.
[25] D.G. Perez, C.S. Fontanetti, Hemocitical responses to environmental stress in invertebrates: a review, Environ. Monit. Assess. 177 (2010) 437–447.

[26] Z. Liu, M. Li, Q. Yi, L. Wang, L. Song, The neuroendocrine-immune regulation in response to environmental stress in marine bivalves, Front. Physiol. 9 (2018) 1456.
[27] I. Efthimiou, G. Kalamaras, K. Papavasileiou, N. Anastasi-Papathanasi, Y. Georgiou, S. Dailianis, et al., ZnO, Ag and ZnO-Ag nanoparticles exhibit differential modes of toxic and oxidative action in hemocytes of mussel *Mytilus galloprovincialis*, Sci. Total Environ. 767 (2021) 144699.
[28] Y. Luo, W.-X. Wang, Immune responses of oyster hemocyte subpopulations to in vitro and in vivo zinc exposure, Aquat. Toxicol. 242 (2022) 106022.
[29] L.M. Oliver, W.S. Fisher, J.T. Winsted, B.L. Hemmer, E.R. Long, Relationships between tissue contaminants and defense-related characteristics of oysters (*Crassostrea virginica*) from five Florida bays, Aquat. Toxicol. 55 (2001) 203–222.
[30] N. Hoeher, A. Koehler, J. Strand, K. Broeg, Effects of various pollutant mixtures on immune responses of the blue mussel (*Mytilus edulis*) collected at a salinity gradient in Danish coastal waters, Mar. Environ. Res. 75 (2012) 35–44.
[31] Y. Wang, M. Hu, Q. Li, J. Li, D. Lin, W. Lu, Immune toxicity of TiO_2 under hypoxia in the green-lipped mussel Perna viridis based on flow cytometric analysis of hemocyte parameters, Sci. Total Environ. 470–471 (2014) 791–799.
[32] F. Wu, H. Falfushynska, O. Dellwig, H. Piontkivska, I.M. Sokolova, Interactive effects of salinity variation and exposure to ZnO nanoparticles on the innate immune system of a sentinel marine bivalve, *Mytilus edulis*, Sci. Total Environ. 712 (2020) 136473.
[33] F. Wu, I.M. Sokolova, Immune responses to ZnO nanoparticles are modulated by season and environmental temperature in the blue mussels *Mytilus edulis*, Sci. Total Environ. 801 (2021) 149786.
[34] A. Pavón, D. Riquelme, V. Jaña, C. Iribarren, C. Manzano, C. Lopez-Joven, et al., The high risk of bivalve farming in coastal areas with heavy metal pollution and antibiotic-resistant bacteria: a Chilean perspective, Front. Cell. Infect. Microbiol. 12 (2022).
[35] I.M. Sokolova, G. Lannig, Interactive effects of metal pollution and temperature on metabolism in aquatic ectotherms: implications of global climate change, Clim. Res. 37 (2008) 181–201.
[36] T.A. Hallman, M.L. Brooks, The deal with diel: temperature fluctuations, asymmetrical warming, and ubiquitous metals contaminants, Environ. Pollut. 206 (2015) 88–94.
[37] C.J. Nin, S. Rodgher, Effect of a temperature rise on metal toxicity for the aquatic biota: a systematic review, Brazilian J. Environ. Sci. 56 (2021) 710–720.
[38] J.B. Jones, Why won't they grow? – inhibitory substances and mollusc hatcheries, Aquac. Int. 14 (2006) 395–403.
[39] E.O. Neokye, X. Wang, K.K. Thakur, P. Quijon, R.A. Nawaz, S. Basheer, Climate change impacts on oyster aquaculture - part I: identification of key factors, Environ. Res. 251 (2024).
[40] E.O. Neokye, X. Wang, K.K. Thakur, P.A. Quijón, R.A. Nawaz, Climate change impacts on oyster aquaculture - part II: impact assessment and adaptation measures, Environ. Res. 259 (2024) 119535.
[41] B. Pogoda, Current status of European oyster decline and restoration in Germany, Humanities 8 (2019) 9.
[42] R. Thurstan, H. McCormick, J. Preston, E. Ashton, F.P. Bennema, A. Bratoš Cetinić, et al., Historical dataset details the distribution, extent and form of lost *Ostrea edulis* reef ecosystems, Sci. Data 11 (2024).
[43] R. Thurstan, H. McCormick, J. Preston, E. Ashton, F.P. Bennema, A. Bratoš Cetinić, et al., Records reveal the vast historical extent of European oyster reef ecosystems, Nat. Sustain. 7 (2024) 1719–1729.
[44] K. Alter, P. Jacobs, A. Delre, B. Rasch, C.J.M. Philippart, M.A. Peck, Oyster larvae used for ecosystem restoration benefit from increased thermal fluctuation, Mar. Pollut. Bull. 198 (2024) 115750.
[45] J. Ellrich, C. Kozian-Fleck, M. Brand, B. Colsoul, B. Pogoda, Ecological reef restoration: consumptive and nonconsumptive interactions among common North Sea predators and European oysters, Front. Environ. Sci. 13 (2025).
[46] V. Sidorenko, S. Rubinetti, A. Akimova, B. Pogoda, A. Androsov, K. Beng, et al., Connectivity and larval drift across marine protected areas in the German bight, North Sea: necessity of stepping stones, J. Sea Res. 204 (2025) 102563.
[47] D.C. Noetzel, B. Colsoul, F. Akcha, N. Briant, J. Le Roy, V. François, et al., Effect of temperature and trace metal exposure on early life stages of European flat oysters and Pacific oysters, Mar. Environ. Res. 211 (2025) 107376.
[48] A.H. Ringwood, J. Hoguet, C.J. Keppler, M.L. Gielazyn, Linkages between cellular biomarker responses and reproductive success in oysters – *crassostrea virginica*, Mar. Environ. Res. 58 (2004) 151–155.
[49] E. Muller, R. Nisbet, H. Berkley, Sublethal toxicant effects with dynamic energy budget theory: model formulation, Ecotoxicology 19 (2010) 48–60.
[50] J. Zhan, T. Sun, X. Wang, H. Wu, J. Yu, Meta-analysis reveals the species-, dose- and duration-dependent effects of cadmium toxicities in marine bivalves, Sci. Total Environ. 859 (2023) 160164.
[51] K. Lika, R.M. Nisbet, A dynamic energy budget model based on partitioning of net production, J. Math. Biol. 41 (2000) 361–386.
[52] L.M. Parker, P.M. Ross, W.A. O'Connor, H.O. Pörtner, E. Scanes, J.M. Wright, Predicting the response of molluscs to the impact of ocean acidification, Biology 2 (2013) 651–692.
[53] H.-O. Pörtner, C. Bock, F.C. Mark, Oxygen- and capacity-limited thermal tolerance: bridging ecology and physiology, J. Exp. Biol. 220 (2017) 2685–2696.
[54] B. Pogoda, P. Boudry, C. Bromley, T.C. Cameron, B. Colsoul, D. Donnan, et al., NORA moving forward: developing an oyster restoration network in Europe to support the Berlin Oyster recommendation, Aquat. Conserv. Mar. Freshw. Ecosyst. 30 (2020) 2031–2037.
[55] D.P. Marisa, R.P. Alan, Metal-induced apoptosis: mechanisms, Mutat. Res. Fund Mol. Mech. Mutagen 533 (2003) 227–241.
[56] M. Valko, H. Morris, M.T. Cronin, Metals, toxicity and oxidative stress, Curr. Med. Chem. 12 (2005) 1161–1208.
[57] P.S. Rainbow, Trace metal bioaccumulation: models, metabolic availability and toxicity, Environ. Int. 33 (2007), 576-501.
[58] B. Foster, S. Grewal, O. Graves, F.M. Hughes Jr., I.M. Sokolova, Copper exposure affects hemocyte apoptosis and *Perkinsus marinus* infection in eastern oysters *Crassostrea virginica* (Gmelin), Fish Shellfish Immunol. 31 (2011) 341–349.
[59] B. Shi, T. Wang, Z. Zeng, L. Zhou, W. You, C. Ke, The role of copper and zinc accumulation in defense against bacterial pathogen in the fujian oyster (*Crassostrea angulata*), Fish Shellfish Immunol. 92 (2019) 72–82.
[60] R.K. Janardhanan, M. Nachev, B. Sures, I.M. Sokolova, Low oxygen stress alters response to sublethal copper exposure without inducing cross-tolerance in the blue mussel *Mytilus edulis*, Aquat. Toxicol. 287 (2025) 107523.
[61] J.A. Coles, S.R. Farley, R.K. Pipe, Alteration of the immune response of the common marine mussel *Mythilus edulis* resulting from exposure to cadmium, Dis. Aquat. Org. 22 (1995) 59–65.
[62] H. Ohkawa, N. Ohishi, K. Yagi, Assay for lipid peroxides in animal tissues by thiobarbituric acid reaction, Anal. Biochem. 95 (1979) 351–358.
[63] D. Tsikas, Assessment of lipid peroxidation by measuring malondialdehyde (MDA) and relatives in biological samples: analytical and biological challenges, Anal. Biochem. 524 (2017) 13–30.
[64] W.C. Sessa, K. Pritchard, N. Seyedi, J. Wang, T.H. Hintze, Chronic exercise in dogs increases coronary vascular nitric oxide production and endothelial cell nitric oxide synthase gene expression, Circ. Res. 74 (1994) 349–353.
[65] K. Walter, C. Schütt, Acid and Alkaline Phosphatase in serum: two-point method, in: H.U. Bergmeyer (Ed.), Methods of Enzymatic Analysis, second ed., Academic Press, 1974, pp. 856–860.
[66] A. Luna-Acosta, H. Thomas-Guyon, M. Amari, E. Rosenfeld, P. Bustamante, I. Fruitier-Arnaudin, Differential tissue distribution and specificity of phenoloxidases from the Pacific oyster *Crassostrea gigas*, Comp. Biochem. Physiol. B Biochem. Mol. Biol. 159 (2011) 220–226.
[67] D. Shugar, The measurement of lysozyme activity and the ultra-violet inactivation of lysozyme, Biochim. Biophys. Acta 8 (1952) 302–309.
[68] Z. Pang, J. Chong, G. Zhou, D.A. de Lima Morais, L. Chang, M. Barrette, et al., MetaboAnalyst 5.0: narrowing the gap between raw spectra and functional insights, Nucleic Acids Res. 49 (2021) W388–W396.
[69] B. Gagnaire, H. Frouin, K. Moreau, H. Thomas-Guyon, T. Renault, Effects of temperature and salinity on haemocyte activities of the Pacific oyster, *Crassostrea gigas* (Thunberg), Fish Shellfish Immunol. 20 (2006) 536–547.
[70] T.J. Green, C. Montagnani, K. Benkendorff, N. Robinson, P. Speck, Ontogeny and water temperature influences the antiviral response of the Pacific oyster, *Crassostrea gigas*, Fish Shellfish Immunol. 36 (2014) 151–157.
[71] C.L. Mackenzie, S.A. Lynch, S.C. Culloty, S.K. Malham, Future Oceanic warming and acidification alter immune response and disease status in a commercial shellfish species, *Mytilus edulis* L, PLoS One 9 (2014) e99712.
[72] G.B. Jones, P. Mercurio, F. Olivier, Zinc in fish, crabs, oysters, and Mangrove Flora and fauna from Cleveland Bay, Mar. Pollut. Bull. 41 (2000) 345–352.
[73] C.Y. Chen, M.-H. Chen, Investigation of Zn, Cu, Cd and Hg concentrations in the oyster of Chi-ku, Tai-shi and Tapeng Bay, Southwestern Taiwan, J. Food Drug Anal. 11 (2003) 32–38.
[74] T.P. O'Connor, G.G. Lauenstein, Status and trends of copper concentrations in mussels and oysters in the USA, Mar. Chem. 97 (2005) 49–59.
[75] G. Lu, A. Zhu, H. Fang, Y. Dong, W.-X. Wang, Establishing baseline trace metals in marine bivalves in China and worldwide: Meta-analysis and modeling approach, Sci. Total Environ. 669 (2019) 746–753.
[76] T. Sun, C. Ji, F. Li, H. Wu, Bioaccumulation and human health implications of trace metals in oysters from coastal areas of China, Mar. Environ. Res. 184 (2023) 105872.
[77] F. Chimienti, M. Aouffen, A. Favier, M. Seve, Zinc homeostasis-regulating proteins: new drug targets for triggering cell fate, Curr. Drug Targets 4 (2003) 323–338.
[78] K. Balamurugan, W. Schaffner, Copper homeostasis in eukaryotes: teetering on a tightrope, Biochim. Biophys. Acta Mol. Cell Res. 1763 (2006) 737–746.
[79] T. Kambe, T. Tsuji, A. Hashimoto, N. Itsumura, The physiological, biochemical, and molecular roles of zinc transporters in zinc homeostasis and metabolism, Physiol. Rev. 95 (2015) 749–784.
[80] R.T. Means, Physiology of copper balance and metabolism, in: R.T. Means (Ed.), Nutritional Anemia: Scientific Principles, Clinical Practice, and Public Health, Cambridge University Press, Cambridge, 2019, pp. 103–110.
[81] W.X. Wang, Y. Yang, X. Guo, M. He, F. Guo, C. Ke, Copper and zinc contamination in oysters: subcellular distribution and detoxification, Environ. Toxicol. Chem. 30 (2011) 1767–1774.
[82] G.W. Bryan, P.E. Gibbs, L.G. Hummerstone, et al., Copper, zinc, and organotin as long-term factors governing the distribution of organisms in the fal estuary in Southwest England, Estuaries 10 (1987) 208–219. https://doi.org/10.2307/1351849.
[83] G.N. Somero, B.L. Lockwood, L. Tomanek, Biochemical Adaptation: Response to Environmental Challenges, from Life's Origins to the Anthropocene, Palgrave Macmillan, 2016, p. 572.
[84] H.C. Davis, A. Calabrese, Survival and growth of larvae of the European oyster (Ostrea edulis L.) at different temperatures, Biol. Bull. 136 (1969) 193–199.
[85] J. Haure, C. Penisson, S. Bougrier, J.P. Baud, Influence of temperature on clearance and oxygen consumption rates of the flat oyster Ostrea edulis: determination of allometric coefficients, Aquaculture 169 (1998) 211–224.

[86] R.C. Newell, L.G. Johson, L.H. Kofoed, Adjustment of the components of energy balance in response to temperature change in Ostrea edulis, Oecologia 30 (1977) 97–110.
[87] C. Eymann, S. Götze, C. Bock, H. Guderley, A.H. Knoll, G. Lannig, et al., Thermal performance of the European flat oyster, Ostrea edulis (Linnaeus, 1758)—explaining ecological findings under climate change, Mar. Biol. 167 (2020) 17.
[88] L. Wang, X. Song, L. Song, The oyster immunity, Dev. Comp. Immunol. 80 (2018) 99–118.
[89] F.-L. Chu, J. La Peyre, Perkinsus marinus susceptibility and defense-related activities in Eastern oysters *Crassostrea virginica*: temperature effects, Dis. Aquat. Org. 16 (1993) 223–234.
[90] K.A. Ashton-Alcox, S.E. Ford, Variability in molluscan hemocytes: a flow cytometric study, Tissue Cell 30 (1998) 195–204.
[91] J. Flye-Sainte-Marie, P. Soudant, C. Lambert, N. Le Goïc, M. Goncalvez, M.-A. Travers, et al., Variability of the hemocyte parameters of *Ruditapes philippinarum* in the field during an annual cycle, J. Exp. Mar. Biol. Ecol. 377 (2009) 1–11.
[92] L. Canesi, G. Gallo, M. Gavioli, C. Pruzzo, Bacteria-hemocyte interactions and phagocytosis in marine bivalves, Microsc. Res. Tech. 57 (2002) 469–476.
[93] C. Cappel, M. Damme, The lysosomal catabolism of nucleic acids—critical regulators of the innate immune system, Nucleic Acids Res. 53 (2025).
[94] A.J. Bune, A.R. Hayman, M.J. Evans, T.M. Cox, Mice lacking tartrate-resistant acid phosphatase (Acp 5) have disordered macrophage inflammatory responses and reduced clearance of the pathogen, Staphylococcus aureus, Immunology 102 (2001) 103–113.
[95] M. Padra, J. Bergwik, A. Adler, G. Marcoux, R.K.V. Bhongir, P. Papareddy, et al., Tartrate-resistant acid phosphatase 5 (TRAP5) promotes eosinophil migration during allergic asthma, Am. J. Respir. Cell Mol. Biol. 73 (2025) 612–622.
[96] L. Delisle, M. Pauletto, J. Vidal-Dupiol, B. Petton, L. Bargelloni, C. Montagnani, et al., High temperature induces transcriptomic changes in *Crassostrea gigas* that hinder progress of ostreid herpesvirus (OsHV-1) and promote survival, J. Exp. Biol. 223 (2020).
[97] J.M. Castro, V.A. Bianchi, E. Felici, J.S. De Anna, A. Venturino, C.M. Luquet, Effects of dietary copper and Escherichia coli challenge on the immune response and gill oxidative balance in the freshwater mussel *Diplodon chilensis*, Environ. Toxicol. Chem. 42 (2023) 154–165.
[98] R.K. Pipe, J.A. Coles, F.M.M. Carissan, K. Ramanathan, Copper induced immunomodulation in the marine mussel, Mytilus edulis, Aquat. Toxicol. 46 (1999) 43–54.
[99] F. Cima, R. Varello, Immunotoxic effects of exposure to the antifouling copper(I) biocide on target and nontarget bivalve species: a comparative in vitro study between *Mytilus galloprovincialis* and *Ruditapes philippinarum*, Front. Physiol. (2023). Volume 14 - 2023.
[100] S. Nicholson, Lysosomal membrane stability, phagocytosis and tolerance to emersion in the mussel *Perna viridis* (Bivalvia: mytilidae) following exposure to acute, sublethal, copper, Chemosphere 52 (2003) 1147–1151.
[101] C. Torres-Duarte, S. Hutton, C. Vines, J. Moore, G.N. Cherr, Effects of soluble copper and copper oxide nanoparticle exposure on the immune system of mussels, *Mytilus galloprovincialis*, Environ. Toxicol. 34 (2019) 294–302.
[102] S. Hojyo, T. Fukada, Roles of zinc signaling in the immune system, J. Immunol. Res. 2016 (2016) 6762343.
[103] H. Gao, W. Dai, L. Zhao, J. Min, F. Wang, The role of zinc and zinc homeostasis in macrophage function, J. Immunol. Res. 2018 (2018) 6872621.
[104] D. Abele, B. Burlando, A. Viarengo, H.-O. Pörtner, Exposure to elevated temperatures and hydrogen peroxide elicits oxidative stress and antioxidant response in the Antarctic intertidal limpet *Nacella concinna*, Comp. Biochem. Physiol. B Biochem. Mol. Biol. 120 (1998) 425–435.
[105] K. Heise, S. Puntarulo, H.O. Pörtner, D. Abele, Production of reactive oxygen species by isolated mitochondria of the Antarctic bivalve *Laternula elliptica* (King and Broderip) under heat stress, Comp. Biochem. Physiol. C Toxicol. Pharmacol. 134 (2003) 79–90.
[106] D. Abele, S. Puntarulo, Formation of reactive species and induction of antioxidant defence systems in polar and temperate marine invertebrates and fish, Comp. Biochem. Physiol. Mol. Integr. Physiol. 138 (2004) 405–415.
[107] J.W. Coleman, Nitric oxide in immunity and inflammation, Int. Immunopharmacol. 1 (2001) 1397–1406.
[108] N.M. Davidson, A. Oshlack, Corset: enabling differential gene expression analysis for de novoassembled transcriptomes, Genome Biol. 15 (2014) 410.
[109] J. Strahl, D. Abele, Nitric oxide mediates metabolic functions in the bivalve *Arctica islandica* under hypoxia, PLoS One 15 (2020) e0232360.
[110] L. Cerenius, K. Söderhäll, Immune properties of invertebrate phenoloxidases, Dev. Comp. Immunol. 122 (2021) 104098.
[111] P. Ferraboschi, S. Ciceri, P. Grisenti, Applications of lysozyme, an innate immune defense factor, as an alternative antibiotic, Antibiotics (Basel) 10 (2021).
[112] S.A. Ragland, A.K. Criss, From bacterial killing to immune modulation: recent insights into the functions of lysozyme, PLoS Pathog. 13 (2017) e1006512.
[113] M. Vincent, R.E. Duval, P. Hartemann, M. Engels-Deutsch, Contact killing and antimicrobial properties of copper, J. Appl. Microbiol. 124 (2018) 1032–1046.
[114] Y. Li, K.W.K. Tsim, W.X. Wang, Copper promoting oyster larval growth and settlement:molecular insights from RNA-seq, Sci. Total Environ. 784 (2021) 147159.
[115] H.F. Prytherch, The role of copper in the setting, metamorphosis, and distribution of the American oyster *Ostrea virginica*, Ecol. Monogr. 4 (1934) 47–107.
[116] C. Ciacci, B. Citterio, M. Betti, B. Canonico, P. Roch, L. Canesi, Functional differential immune responses of *Mytilus galloprovincialis* to bacterial challenge, Comp. Biochem. Physiol. B Biochem. Mol. Biol. 153 (2009) 365–371.